2020-01-0613

Knock, auto-ignition and pre-ignition tendency of Fuels for Advanced Combustion Engines (FACE) with ethanol blends and similar RON.

Author, co-author (Do NOT enter this information. It will be pulled from participant tab in MyTechZone)

Affiliation (Do NOT enter this information. It will be pulled from participant tab in MyTechZone)

Abstract:

Researchers have known about a higher pre-ignition frequency of alcohol fuels for several decades now. Several studies, assessing the effect of ethanol addition on stochastic pre-ignition, have shown contradicting observations. Researchers at FEV observed an increase in pre-ignition frequency with an increase in ethanol concentration, however the pre-ignition events at high ethanol content did not lead to super-knock. Most of the studies have used varying ethanol fraction in a common base-fuel, thereby varying the auto-ignition tendency of the blend. In the current study, the effect of ethanol addition on FACE (Fuels for Advanced Combustion Engines) gasolines is assessed. Five different FACE gasolines (FACE A, C, I, J and G) were used for the study. Ignition delay time of varying ethanol fractions in FACE gasolines was measured in an Ignition Quality Tester (IQT), following ASTM 6890. The measurements showed that 13% ethanol (v/v) is needed for FACE A and C, while 27% ethanol (v/v) is needed for FACE I and J to match the ignition delay time of FACE G fuel. The five blends were tested in a Co-operative Fuel Research (CFR) engine in Homogeneous Charge Compression Ignition (HCCI) and Spark Ignition (SI) combustion mode. The experiments showed similar auto-ignition and knocking tendency for the five blends. After that, the pre-ignition tendency of the blends was assessed in a supercharged AVL engine. In general, increasing ethanol content led to higher pre-ignition frequency. Moreover, the effect of ethanol on increasing pre-ignition frequency was dependent on the base-fuel into which ethanol was added. For the same ethanol fraction added, base-fuels with higher aromatic content showed higher pre-ignition frequency.

Introduction:

Pre-ignition has been one of the most mysterious issues plaguing modern downsized spark-ignited engines. Appositely called stochastic pre-ignition, it refers to an abnormal combustion phenomenon, wherein both auto-ignition and combustion occur earlier than spark timing and usually from a source, other than the spark plug [1-3]. Lubricant oil-fuel droplets and deposits have been attributed to triggering pre-ignition at high load operation, usually at low engine speeds. Some recent studies in on-road vehicles have also shown pre-ignition frequency peaking at relatively higher engine speeds (3000-4000 rpm) [4].

Several researchers have investigated the fuel effects on pre-ignition frequency. Pre-ignition in earlier times (before 2005) was mostly attributed to hot engine component surfaces and deposits. Experiments conducted by Downs *et al.* used a pre-igniter for rating various hydrocarbons for their pre-ignition frequency. The electrical power required to initiate a pre-ignition event, often detected by an ion-current sensor, was used to give a pre-ignition rating to the fuels tested [5, 6]. In general, alcohol fuels performed worse in terms of pre-ignition frequency. Methanol was slightly more pre-ignitive compared to ethanol.

In 1945, Zeldovich [7] proposed that a flame kernel larger than a critical diameter leads to a propagating flame. The critical radius (R_f) depends on Lewis number (Le) and Zeldovich number $\beta = E(T_b - T_u)/RT_b^2$, where E, T_u, T_b and R refer to the activation energy, unburned temperature, burned temperature and universal gas constant respectively, as shown by Eq. 1.

$$\frac{R_f}{\delta} = \exp\frac{1}{2}\beta\left(1-\frac{1}{Le}\right) \quad \text{.....(1)}$$

where δ is the flame thickness, which depends on the flame speed as given below by an empirical Eq. 2.

$$\delta = \frac{\mu}{\rho S_L} = \frac{\mu_0}{\rho_0 S_{Lo}}\left(\frac{P}{P_0}\right)^{m-1}\left(\frac{T}{T_0}\right)^{1.5-n} \quad \text{.....(2)}$$

Fuels with higher flame speed have a lower flame thickness, leading to a smaller critical diameter. For a randomly distributed size of mobile or surface flame kernels in a combustion chamber, the probability of a flame kernel to develop into propagating flame, and lead to pre-ignition will be higher for a fast burning fuel. For eg. Hydrogen has relatively high flame speed and is known to be very prone to pre-ignition. A high correlation between the laminar flame speed and pre-ignition rating of several fuels was reported in 2012 by Kalghatgi [8-10].

Hülser *et al.* [11] optically visualized pre-ignition for several biofuel molecules. Ethanol showed very high pre-ignition frequency, which was mostly attributed to the poor mixture formation, owing to a larger mass of fuel injected and higher latent heat of vaporization. Fewer of these pre-ignition events started at the spark plug, apparently due to the charge cooling provided by ethanol spray impingement on the spark plug. In 2016, Mayer *et al.* [12] investigated the effect of ethanol addition on pre-ignition using similar RON blends with ethanol fraction ranging from 0% to 50% (v/v). They observed that pre-ignition frequency decreased going from E0 to E30 (attributed to increased charge cooling effect), while pre-ignition increased tremendously for E50 (attributed to increased fuel-wall impingement). The reduction in pre-ignition frequency has also been reported by Martin *et al.* [13].

The researchers also splash blended E30 with more ethanol, thereby forming E50specE30 fuel. This blend (higher RON compared to E50) showed increased pre-ignition frequency compared to E30, but slightly lower than E50. The observations helped deduce the effect of the base-fuel as well as RON values on pre-ignition and super-knock separately. Researchers at FEV [14] used varying levels of ethanol fraction in a

gasoline base-fuel. They observed that increasing ethanol fraction (v/v) in gasoline increased the pre-ignition frequency [14].

The effect of various hydrocarbon classes has also been investigated extensively in the past. Most of those publications attempted correlating the tail-end of the distillation curve of the gasoline (T_{90}: the temperature at which 90% of the volume has evaporated) with the pre-ignition frequency [1, 2, 15, 16]. Generally, a less volatile fuel led to higher pre-ignition frequency [12]. Moreover, an increasing fraction of olefins and aromatics have been shown to increase the pre-ignition frequency. While the presence of aromatics reduces the volatility of the gasoline, olefins increased the surface ignition tendency of the fuel [17-19]. The effect of aromatics on pre-ignition frequency is also documented well in [6, 19, 20]. Most publications observed an increase in pre-ignition frequency with an increase of aromatic content in the fuel blends. This effect is attributed to a reduction in volatility as well as an increase in deposit formation tendency of the fuel as aromatics content increases. However, research by Constanzo *et al.* has shown a lack of correlation between deposit formation tendency from aromatic fuels and pre-ignition frequency in modern turbocharged engines [2].
The existing literature does not inform about the effect of ethanol addition in varying base-fuel composition on pre-ignition frequency. The current research aims to fill this gap by investigating five fuels with varying ethanol fractions, as well as varying base-fuel composition. The methodology followed in this work allows attributing the observations to the differences in ethanol fraction as well as base-fuel composition.
The experiments were conducted with five different fuel blends. FACE fuels with varying ethanol fraction are tested for (a) ignition delay time in IQT, (b) auto-ignition and knocking tendency in a CFR engine, and (c) pre-ignition frequency in a modern architecture AVL engine. The work provides comprehensive data on the effect of fuel composition on auto-ignition, knocking and pre-ignition tendency.

Methodology:

The experiments were conducted in three steps. Given below are the methodologies followed for each step.

1. Ignition Quality Tester (IQT)

The KR-IQT (KAUST Research- Ignition Quality Tester) was used to ascertain the ethanol fraction needed in FACE fuels to achieve similar ignition delay time (IDT) [21]. Previous studies have observed a high correlation between IDT and the standard RON values [22]. A resolution of 1% (v/v) was deemed good enough to match the approximate IDT of the five blended fuels. IQT is a constant volume combustion chamber, with a pintle type nozzle for fuel injection at 225 bar. The chamber is filled with air up to 22.4 bar pressure. The chamber temperature is fixed such that injecting n-heptane gives an IDT of 3.78±0.03 ms. For the current study, n-heptane showed an IDT of 3.80 ms at chamber temperature of 579°C. The experiments were conducted following ASTM D6890, wherein 15 pre-injections are followed by 32 injections [23]. The average of the 32 injections is denoted as the IDT. FACE G has the highest RON, hence FACE C and FACE I were blended with ethanol to match the IDT of FACE G. To compare the effect of base-fuel, FACE A and FACE J were blended with the same ethanol volume fraction as FACE C and FACE I, respectively. FACE A and FACE C naturally require lower ethanol addition to match the IDT of FACE G, compared to FACE I and FACE J fuels.

2. CFR engine experiments

CFR is a standard engine used for measuring RON and MON ratings for gasoline fuel [24, 25]. In the current study, the methodology was modified to operate the engine in conventional spark-ignited (SI) mode as well as in homogeneous charge compression ignition (HCCI) mode. The engine is made by Waukesha and has a variable compression ratio design, ranging from 4 to 15.5. A port fuel injector has been used instead of a carburetor. The air temperature was maintained at 52°C, and engine speed was fixed at 600 rpm, both values being standard for RON tests. A thermocouple 3.5 cm upstream of the fuel injector was used to measure the intake air temperature. The injection pressure for the port fuel injector was set at 6 bar. The duration of injection was varied to fix the lambda = 3 for HCCI conditions and lambda = 1 for SI conditions, as measured by the lambda sensor downstream of the exhaust valve. The water-cooling line was maintained at 95°C throughout the experiments. For the HCCI experiments, the compression ratio was varied to achieve auto-ignition, such that the CA50 was at TDC (or 0 CAD aTDC) for each fuel. The methodology is similar to HCCI#1 used previously in [26]. In the case of SI combustion mode, the compression ratio was fixed at 6.5, and the spark timing was advanced from 0 CAD aTDC to knock limited conditions, with a step of 3 CAD. Details on the engine hardware are given in Table 1.

Table 1: Specifications for a CFR engine used for auto-ignition and knock study.

Engine Type	Single Cylinder CFR
Injection System	Port Fuel Injection
Bore	82.6 mm
Stroke	114.3 mm
Connecting Rod	254.0 mm
Compression Ratio	Variable from 4 – 15.5
Speed	600 rpm
Spark Timing	Variable
Intake Air Temperature	52±2°C
Lambda	1 (SI) and 3 (HCCI)

3. Pre-ignition engine experiments

An AVL pre-ignition engine was used to test the pre-ignition frequency of the five blends. The test method used in the current experiments is similar to the one used by the authors in previous publications, with the difference that a variable spark timing was used in the current experiments [27, 28]. The spark timing for each fuel was such that the average knock intensity of normal combustion cycles was ~ 0.5 bar. The engine is equipped with a centrally mounted direct injector with an injection pressure of 130 bar. The coolant temperature was maintained at 80°C and the intake air temperature was maintained at 30°C. The start of injection occurs at -300 CAD aTDC (in the intake stroke). 15,000 cycles were recorded in each batch and 8 such batches were recorded, amounting to a total of 120,000 cycles for each fuel blend. The results are shown in % (number of pre-ignition events per 100 cycles). Robust statistics was used to detect pre-ignition events, allowing a lower impact of outliers on mean and standard deviation calculations [29]. The start of combustion (CA05) was used as a

marker for pre-ignition events and pre-ignition frequency is calculated based on eq. (3) given below:

$$PI\ frequency = \#\left[CA05 < \left(R\overline{CA05} - 5\sigma(CA05)\right)\right] \text{ ….…..……(3)}$$

where $R\overline{CA05}$ refers to the mean and $\sigma(CA05)$ refers to the standard deviation of all CA05 data. The details of the engine hardware are given in Table 2. The engine experiments were run at a fixed engine speed of 2000 rpm. It was ensured that no deposits have accumulated over the runtime and lubricant oil was changed at regular intervals.

Table 2: Specifications for the AVL engine used for pre-ignition study.

Engine Type	AVL Single Cylinder
Displacement Volume	454 cc
Stroke	86
Bore	82
Connecting Rod	114
Compression Ratio	9.5:1
Valvetrain	4 valve – DOHC
Cylinder head	Pent roof

Fuels used:

As mentioned previously, five different FACE fuels were used in the current study. The five fuels can be grouped into three categories, FACE G has high RON and S; FACE A and FACE C have mid-RON and low S; while FACE I and FACE J have low-RON and S. The octane number values are given in Table 3. Apart from the difference in RON and MON, these fuels have different compositions. Figure 1 shows results from DHA analysis done by CRC. It can be observed that FACE G and FACE J have high aromatic content. FACE G and FACE I have high olefinic content, while the naphthenic mass fraction follows the order: FACE G>FACE I>FACE J. FACE A and FACE C are mostly paraffinic, with FACE C having slightly higher aromatic and olefinic content in comparison. Other relevant properties of the FACE fuels are given in Table 4. The distillation curves for the five FACE fuels is shown in Figure 2. Distillation curves were obtained by ASTM D86 standards [30].

Table 3. Octane Number and Sensitivity of five base-fuels used in the current study.

Base fuel	RON	MON	S
FACE G	96.5	84.8	10.7
FACE A	83.9	83.5	0.4
FACE C	84.3	83.0	1.3
FACE I	70.0	69.5	0.5
FACE J	73.8	70.5	3.7

Table 4: Properties of five base-fuels used in the current study

Property	FACE G	FACE A	FACE C	FACE I	FACE J
Reid Vapor Pressure (psi)	7.25	8.05	7.45	7.60	7.50
API Gravity	54.55	74.95	73.30	74.40	59.10
Density (g/ml)	0.760	0.685	0.691	0.697	0.742
Net heat of combustion (MJ/kg)	43.27	44.77	44.79	44.72	43.57
H (wt %)	13.30	16.01	15.47	15.86	13.76
C (wt %)	86.70	83.99	84.53	84.14	86.24
Sulphur Content (ppm)	22	6	4	2	2

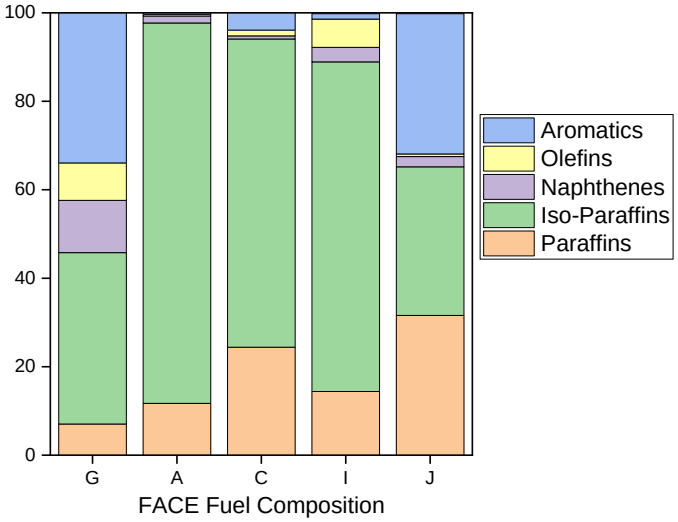

Figure 1. Detailed Hydrocarbon Analysis (DHA) of five base-fuels used in the current study.

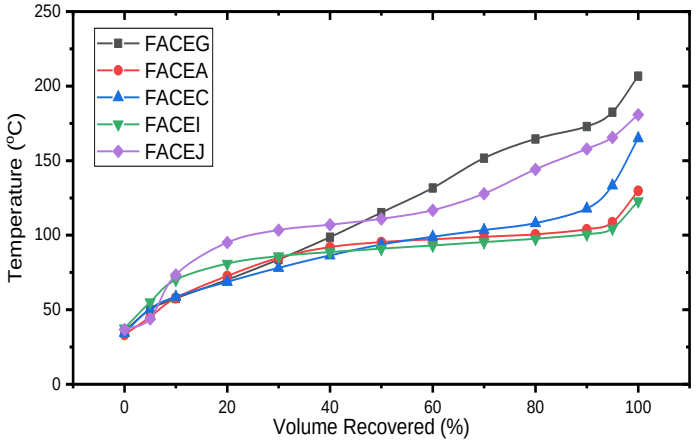

Figure 2: Distillation data (by ASTM D-86) for five base-fuels used in the current study.

Results and Discussions:

Ignition Delay Measurements in IQT:

Experiments were conducted in an IQT with varying ethanol fraction. Ethanol was added to FACE I and FACE C to match the IDT of FACE G. The measured IDT values are shown in figure 3. The average of 32 injections is shown in the figure along with the standard deviation as the error bar. Based on the measured values in Figure 2, 13% (v/v) ethanol is blended in FACE C and FACE A, while 27% (v/v) ethanol is blended in FACE I and FACE J gasolines. Although, the IDT of FACE A and FACE J may not have matched those of FACE C and FACE I respectively, the choice to keep ethanol fraction fixed was to attribute the difference in observations to the base-fuel composition and not to changes in ethanol fraction. With regards to the effect of

ethanol addition alone, figure 3 shows an increase in IDT as ethanol is added to FACE I fuel. [22, 31] showed a correlation between octane numbers and experimentally measured IDT values. The values shown in Figure 3 correspond to the non-linear octane boosting tendency of ethanol. [26, 32] suggest that this non-linear octane boosting tendency arises from the radical scavenging nature of ethanol, which suppresses the low-temperature reactivity responsible for engine knock.

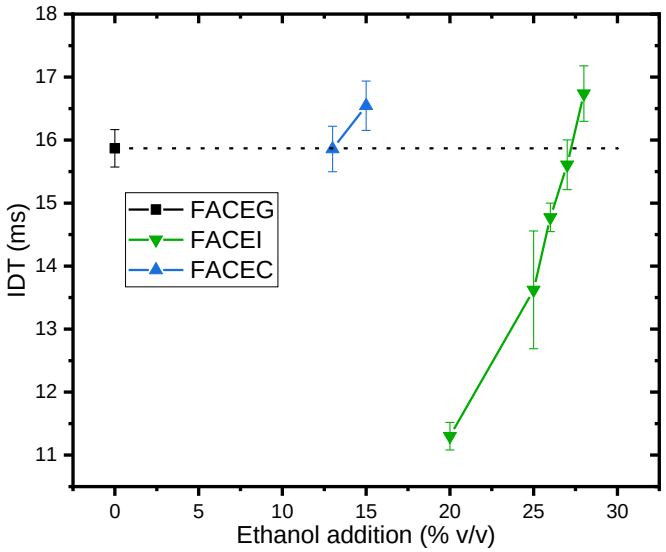

Figure 3: Ignition delay times, as measured in an IQT for three FACE fuels and their ethanol blends

Distillation data ASTM D-86:

The distillation data for the five blends is now acquired using a MiniDistillation unit, following the ASTM D-86 standard [30]. The data is collected three times and the average value of the three runs is reported in figure 4. Plateauing of the distillation curve in the range of 50 to 75°C for ethanol blends can be observed. Ethanol molecule forms an azeotrope with the hydrocarbon molecules considered in the study, leading to flattening in the distillation curve. The azeotrope formation leads to a reduction in area under the distillation curve, compared to pure FACE fuels, resulting in lower drivability index (DI) in some cases [33]. DI is given in Eq. (4) and depends on the temperature at which 10%, 50%, and 90 % of fuel has evaporated [34].

$$DI = 1.5T_{10} + 3.0T_{50} + 1.0T_{90} + 1.33[EtOH\ vol\%] \quad \text{.....(4)}$$

Table 5 shows the drivability index values for blended fuels. A high drivability index signifies a smooth and reliable response to throttle opening and closing at engine start, warming up and running.

Table 5: Drivability Index of five fuel blends.

FACEG	FACEA13E	FACEC13E	FACEI27E	FACEJ27E
645	457	473	451	554

The azeotrope further results in higher volatility of the gasoline blend as ethanol fraction is increased [35]. The extent of azeotropic mixture formation is also observed to depend on the base-fuel composition, and not only on the ethanol fraction added. For example, at 27% ethanol addition, FACE I and FACE J, showed higher extent of azeotropic behavior, compared to 13% ethanol added to FACE A and FACE C. For same ethanol fraction, while azeotropic behavior was observed until ~60% volume evaporated for FACE J, it was observed until ~90% volume evaporated for FACE I blend.

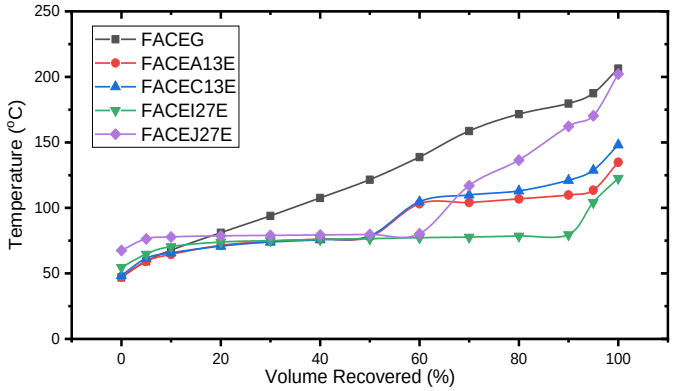

Figure 4. Distillation curve for five fuel blends investigated in the current study.

It must be noted that for most fuels, the tail end of the distillation curve is not heavily affected by ethanol addition. Several pre-ignition studies have focused on T_{90} being critical to the pre-ignition behavior of fuel [1, 2, 19]. The ethanol fraction present at each recovery point may be critical. For example, if T_{90} is critical to pre-ignition frequency, it should mean that the triggering particles are composed of compounds in the tail end of distillation. It was found that the ethanol fraction within each recovery point (T_{10} to T_{90}) varies significantly [36]. Balabin *et al.* observed that the mid-fractions of the distillation carry most of the ethanol, while negligible ethanol was recovered at T_{85} and above [36]. Hence, the effect of ethanol addition and heavier components can be isolated. This may not have a substantial effect on port injection experiments conducted in the CFR engine but may affect pre-ignition frequency, as recorded in the direct-injected AVL engine.

HCCI Experiments in CFR Engine

Waqas et al [26, 37] reported synergistic auto-ignition suppression of ethanol added to FACE gasolines, when operating a CFR engine in HCCI mode. The authors used varying level of ethanol in FACE A, FACE I and FACE J. A non-linear blending behavior was observed, signifying a more suppressed auto-ignition tendency at lower ethanol concentration (by v/v), compared to blends at higher ethanol concentration (by v/v). Ethanol is known to suppress low-temperature reactions by acting as a radical scavenger, which leads to a greater auto-ignition suppression in HCCI combustion [32]. In the current study, the intake air temperature and engines speed were fixed at 52°C and 600 rpm respectively, same as in RON tests. The auto-ignition phasing was fixed, and the compression ratio required to achieve a fixed auto-ignition phasing was noted. The pressure traces from the final compression ratios are shown for the five blends in figure 5. The compression ratio required to achieve auto-ignition phasing at TDC is shown in figure 6.

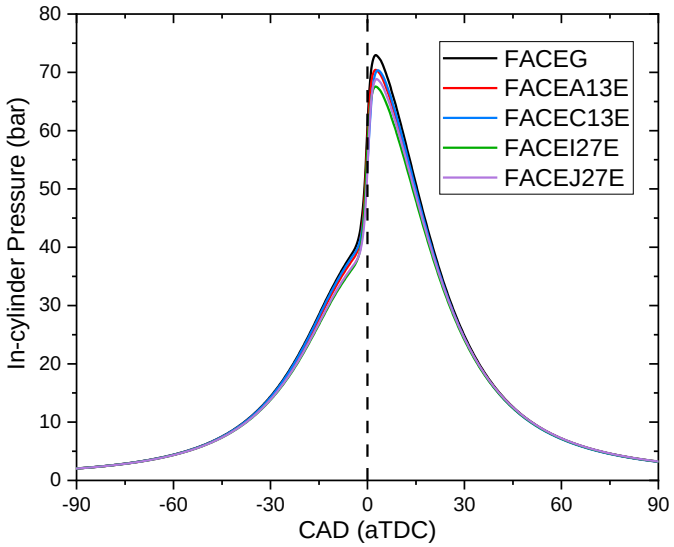

Figure 5. In-cylinder pressure data for five fuel blends investigated in the current study.

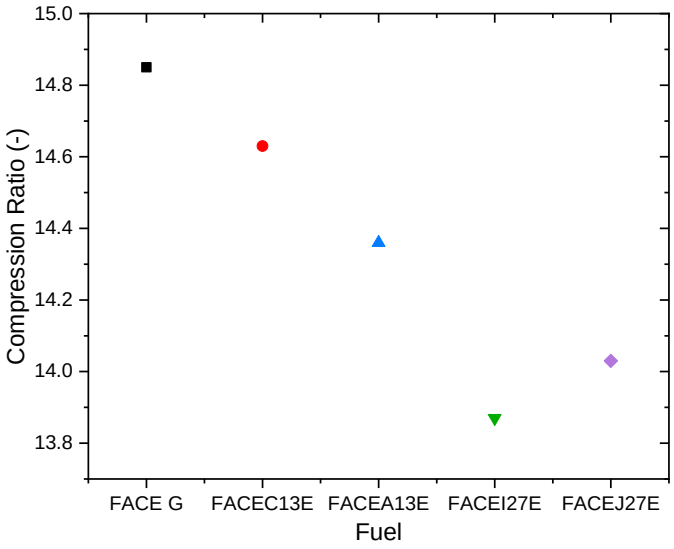

Figure 6. Compression ratio required by five fuel blends to achieve similar combustion phasing in HCCI mode of engine operation.

Although the three out of five blends showed similar ignition delay times in IQT, there is a slight difference in auto-ignition tendency in a homogenous environment. FACE G showed the lowest auto-ignition tendency, followed by FACE A and FACE C blended in 13% ethanol, followed by FACE I and FACE J blended in 27% ethanol.

As opposed to spray combustion in an IQT, these experiments have very low charge stratification at the time of auto-ignition. The difference between the two observations (IQT and HCCI experiments) highlights the effect of fuel stratification and charge cooling on the auto-ignition tendency of ethanol blends. Seminal work in this area has been done by Dec and co-workers [38, 39]. The authors showed that fuels exhibiting prominent NTC behavior showed a higher sensitivity to equivalence ratio variations. A higher equivalence ratio sensitivity allowed sequential auto-ignition extending the load range for LTGC engines. In contrast, fuels were injected in a constant volume at 22.4 bar 579 ºC in the IQT experiments, where the fuel stratification was high. As will be seen in chemical kinetic simulations in this work, FACE I and FACE J with 27% ethanol showed slightly less prominent NTC behavior relative to other blends.

SI Experiments in CFR Engine

Spark-ignited engine experiments were conducted at a fixed compression ratio of 6.5 in the CFR engine. The spark timing was advanced from 0 CAD aTDC with a step of 3 CAD. The knock intensity reported in this work is defined as the difference between the maximum and the minimum of the pressure fluctuations from five-point moving averaged pressure. The average knock intensities over 200 cycles are reported in figure 7. The knock tendency of the five fuels is similar, which is expected from the previous observations made in IQT and HCCI experiments. FACE G, 13% ethanol in FACE A and FACE C, and 27% ethanol in FACE I showed similar knocking tendency, while FACE J with 27% ethanol showed relatively higher knocking tendency for all spark timings.

The three observations together can be used to see the effect of stratification and flame travel. In SI engine experiments, knock is auto-ignition of end-gas ahead of a deflagrative flame front. Therefore the disparity in the observations between SI and HCCI experiments can be attributed to the change in lambda (= 3 for HCCI versus =1 for SI mode) and the effect of flame (sequential auto-ignition of the bulk mixture in HCCI versus auto-ignition of end-gas ahead of the flame front).

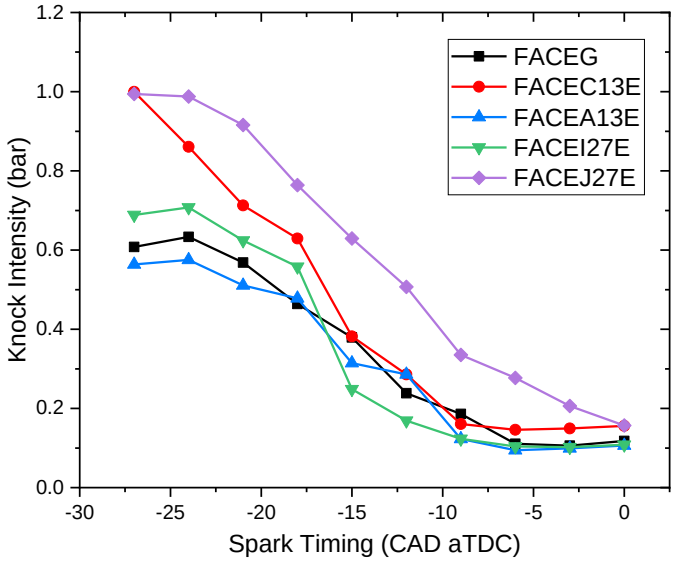

Figure 7. Knock intensity is shown as a function of spark timing at RON-like conditions for five fuel blends investigated in the current study.

Pre-ignition Experiments in AVL Engine

To assess the pre-ignition frequency, experiments were conducted in an AVL engine with an intake air pressure 2.1 bar and intake air temperature 30°C. The number of pre-ignition events (per 100 cycles) is shown in figure 8. FACE G and FACE A with 13% (v/v) ethanol showed similar pre-ignition frequency. FACE C with 13% (v/v) ethanol showed relatively high pre-ignition frequency in comparison.

With the further addition of ethanol (27%), pre-ignition frequency increased further. In general, pre-ignition frequency increased with increasing ethanol fraction. Apart from the chemical effect of ethanol (driven by high flame speed), this increase in pre-ignition may also be attributed to the increased mass of fuel injected for maintaining the stoichiometric air-fuel ratio, as ethanol fraction increased. Among FACE C and FACE A, ethanol fraction did not have a huge impact on the pre-ignition frequency. FACE A is composed almost entirely of saturated molecules (paraffins, iso-paraffins, and naphthene), while FACE C has 3.9% aromatics and 1.3% olefins. FACE G showed minimum pre-ignition frequency, although the composition has a maximum aromatic and olefinic fraction. The interaction between ethanol fraction and base-fuel may be critical to pre-ignition frequency. Among FACE I and FACE J, FACE J showed higher pre-ignition frequency, which agrees with the relatively high aromatic fraction of FACE J (figure 1). Secondly, looking at the T_{90} from the distillation curve in Figure 3, FACE G and FACE J had similar values, while their pre-ignition frequency is very different. FACE I blend had minimum T_{90} while it showed relatively high pre-ignition frequency. Overall, the tail end of the distillation curve and the base-fuel composition alone, do no explain the pre-ignition frequency. However, base-fuel composition, coupled with ethanol fraction correlates with pre-ignition frequency observed in the AVL engine.

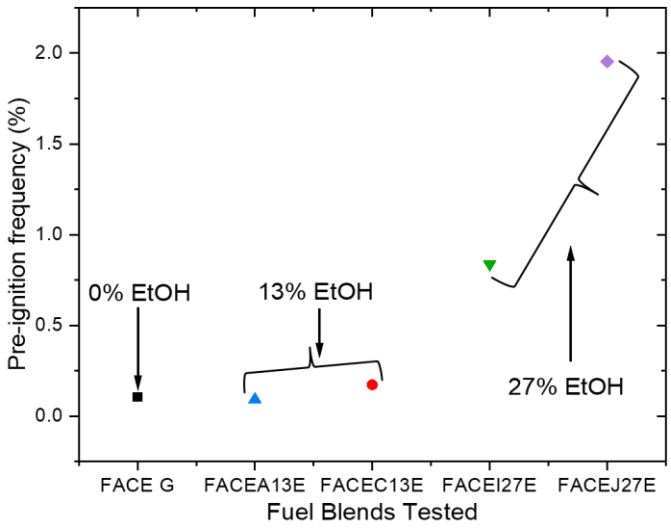

Figure 8. Pre-ignition frequency of five fuel blends investigated in the current study.

Chemical Kinetic simulations:

In order to investigate the resistance of the five fuel blends over a range of temperatures, chemical kinetic simulations were conducted in ChemKin solver using a homogeneous batch reactor module [40]. The mechanism used for these calculations has been tested over engine operating conditions [41, 42]. Surrogates were formulated for respective FACE fuels and are shown in Table 5 [41-43]. The energy equation was solved for varying initial temperature and pressure conditions. Figure 9 shows the results from calculations. As expected, the simulations do a good job of replicating the chemical auto-ignition behavior of the fuel blends, showing similar ignition delay times in the wide range of temperature that covers low and high-temperature chemistry (700-1000 K). Reactivity in the negative temperature coefficient region (NTC) has previously been correlated with fuels' knocking tendency and octane number [32, 44]. Fuels with higher ethanol fraction (FACE I and FACE J with 27% ethanol) showed slightly lower reactivity in the NTC regime, signaling a higher octane-sensitivity (S).

Table 5: Surrogate formulation used for five fuel blends investigated in this study.

	FACE J	FACE I	FACE G	FACE A	FACE C
Molecular Mass	94.67	95.45	99.7	97.8	97.2
Density (kg/L)	0.742	0.697	0.76	0.685	0.691
Surrogate	mol%				
n-Butane	0	0	7.6	10	18.4
2-methylbutane	0	11	9.5	12	5
2-methylhexane	0	27	9.8	10.3	4.7
Cyclopentane	0	6	15.3	0	0
1,2,4-Trimethylbenzene	0	4	21.1	0	0
1-Hexene	0	6	8.1	0	0
n-Heptane	33.9	12	0	7	12.5
iso-Octane	45.2	34	18	60	54.6
Toluene	0.2	0	10.6	0	4.8

The results shown in figure 9 consider only the chemical reactivity and can be used to isolate the chemical auto-ignition tendency from the effect of physical properties (charge cooling owing to the latent heat of vaporization), which play a major or minor role in the above methodologies, depending on stratification levels.

Discussions:

Chemical kinetic simulations suggest that the five blends perform similarly in terms of chemical auto-ignition resistance. This is representative of auto-ignition tendency in a homogenous environment. An HCCI engine operation comes close to such an ideal case, but the in-cylinder temperature is reliant on the charge cooling effect provided by the fuel. As observed in figure 6, all fuels showed similar auto-ignition tendency within 1 compression ratio (13.8-14.8).

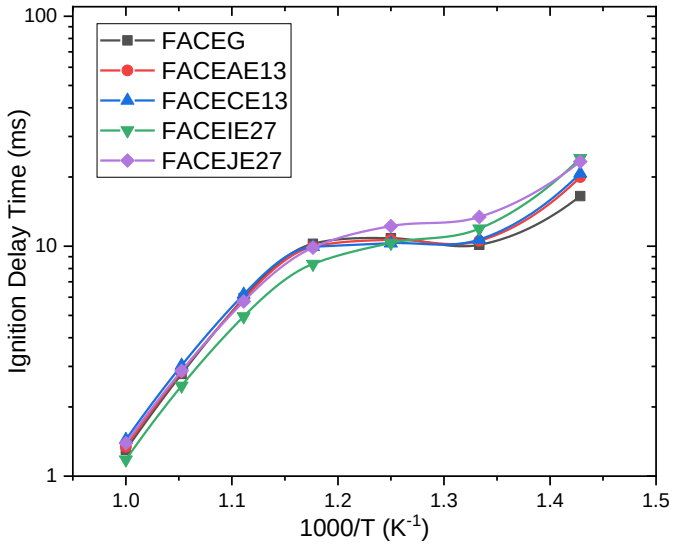

Figure 9: Ignition delay time of the five fuel blends plotted on a log scale versus the inverse of temperature.

Use of ethanol in other injection strategies and effect on pre-ignition:

In contrast to preceding sections that investigated ethanol in blends with FACE fuels, the current section looks at data collected previously for ethanol injection; separately, via port injector or direct injector. Two methodologies are shown here, with regard to their pre-ignition tendency: 1) using the port injection of ethanol in the Octane-on-Demand concept, and 2) using a second direct injection of ethanol late in the compression stroke. Figure 11 shows a probable sequence of events leading to pre-ignition followed by super-knock.

1. Fuel spray hits the wall. Fuel mixes with oil film on cylinder liner, forming a droplet.

2. The droplet may be launched into the combustion chamber due to inertial forces near the top dead center.

3. The wandering droplets get heated (and burned) during the normal combustion cycle.

4. Most droplets are scavenged out of the engine during the exhaust stroke.

5. Due to the non-ideal scavenging process, a small fraction of burned mixture, carrying heated (and burned) droplets, remains inside the engine.

6. The hot (or burned) droplet may trigger a pre-ignition event if the atmosphere (fuel-air mixture around the droplet) is reactive enough [45]. The processes 1 to 6 are shown schematically in figure 10.

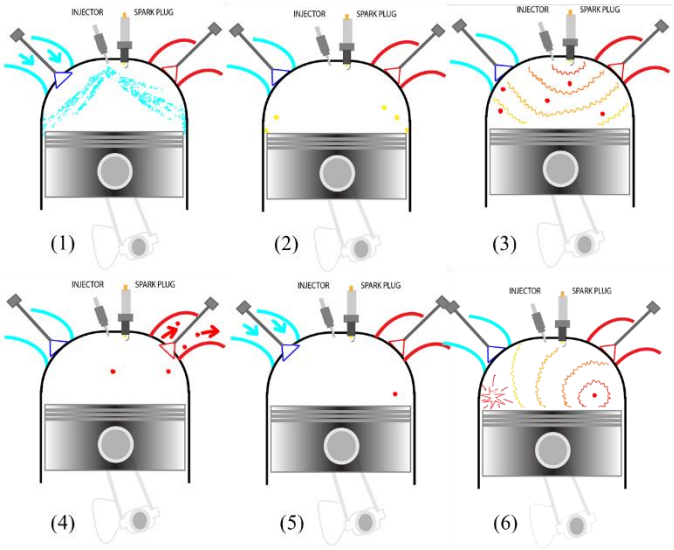

Figure 10: Conceptual framework for mechanism triggering pre-ignition event in the spark-ignited engine.

Octane-on-Demand concept uses low-octane gasoline (light naphtha injected via direct injector) at low load operation, and ethanol is separately added via port fuel injector when the engine is knock limited [46-48]. Such strategies have shown a well-to-wheel GHG emission reduction of up to 30% [49-52].

Intake air pressure is increased until the engine is knock limited when operating with light-naphtha-only. At such a condition, a fraction of light naphtha is replaced by ethanol, allowing maximum brake torque (MBT) spark timing to be achieved. Figure 11 shows IMEP plotted against the fraction of ethanol (injected via port fuel injector) displacing light naphtha.

Expectedly, a negligible amount of ethanol is needed at low load operation (intake air pressure up to 0.7 bar, IMEP up to 7 bar) and more ethanol is needed to achieve MBT timing as intake pressure increases (engine is more knock limited at higher loads). Consider the case of intake pressure 1.3 bar in figure 11. Pre-ignition is observed at a low IMEP of 13 bar at 0% ethanol operation (as shown by shaded area). At this condition, a large fuel mass is injected via direct injection route, leading to a higher probability of generation of oil-fuel droplets from fuel impingement on liner (step 1 in figure 10). These oil-fuel droplets can form pre-ignition precursors in the subsequent cycle.

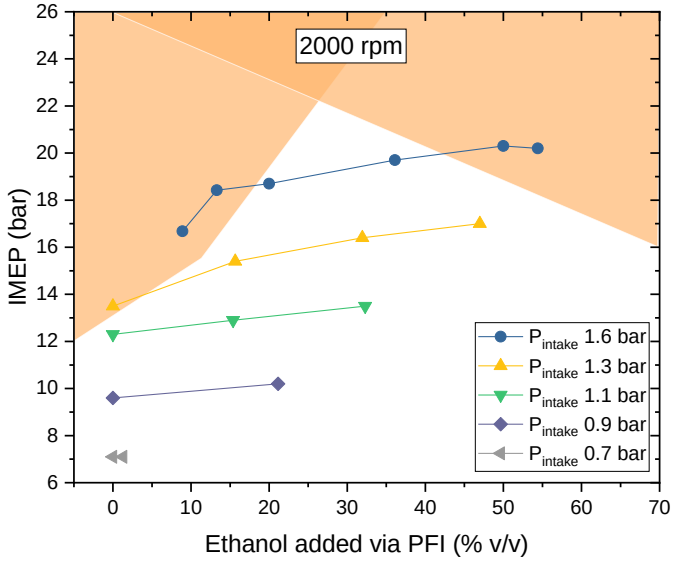

Figure 11: IMEP is plotted against volume fraction of ethanol displacing light naphtha to suppress knock, for increasing intake air pressure. Engine operation limited by pre-ignition is shown in an orange shaded area [52].

As the mass of ethanol injected via PFI increases, the direct-injected fuel mass impinging the liner decreases, leading to fewer precursor generation. This leads to a region of pre-ignition free operation as ethanol is added.

For intake pressure 1.6 bar, pre-ignition limits on low ethanol fraction can be attributed to high fuel-wall impingement. At mid ethanol fraction (20 to 45% (v/v)), the liquid impingement is not critically high. Therefore pre-ignition free operation is possible. As ethanol fraction increases further, the mass of fuel injected via PFI reaches a critical value when it can dilute the oil film on the liner via liquid fuel entering the combustion chamber on the back of the intake valve. Secondly, as seen in this study, ethanol has a higher pre-ignition frequency. Therefore, pre-ignition frequency increases with increasing ethanol in the charge. Consequently, at intake air pressure of 1.6 bar, pre-ignition re-emerges at a high ethanol fraction (50% (v/v) and above). Overall, splitting the injection in the Octane-on-Demand helps in suppressing pre-ignition, but pre-ignition re-emerges at high ethanol fractions.

In the second strategy, ethanol is injected late in the compression stroke [27]. Ethanol has a relatively high latent heat of vaporization and injecting ethanol in compression stroke is an effective way to cool the bulk mixture. Experiments were performed with gasoline as primary fuel injected early in intake stroke (-300 CAD aTDC) and small ethanol quantity is injected late in the compression stroke (-30 CAD aTDC). This allows reducing bulk mixture properties, at the time when pre-ignition could have occurred (pre-ignition events occur between -17 to 0 CAD aTDC). Figure 12 shows the effectiveness of late split injection strategy and the effect of using ethanol in the late split pulse. Only a couple of pre-ignition events (with low knock intensity) can be observed when using split injection (red data points in figure 12a). Replacing the gasoline in late split injection with ethanol, pre-ignition reduces tremendously, as observed in figure 12b. Neglegible pre-ignition frequency is achieved with just 2 mg ethanol injected at -30 CAD aTDC.

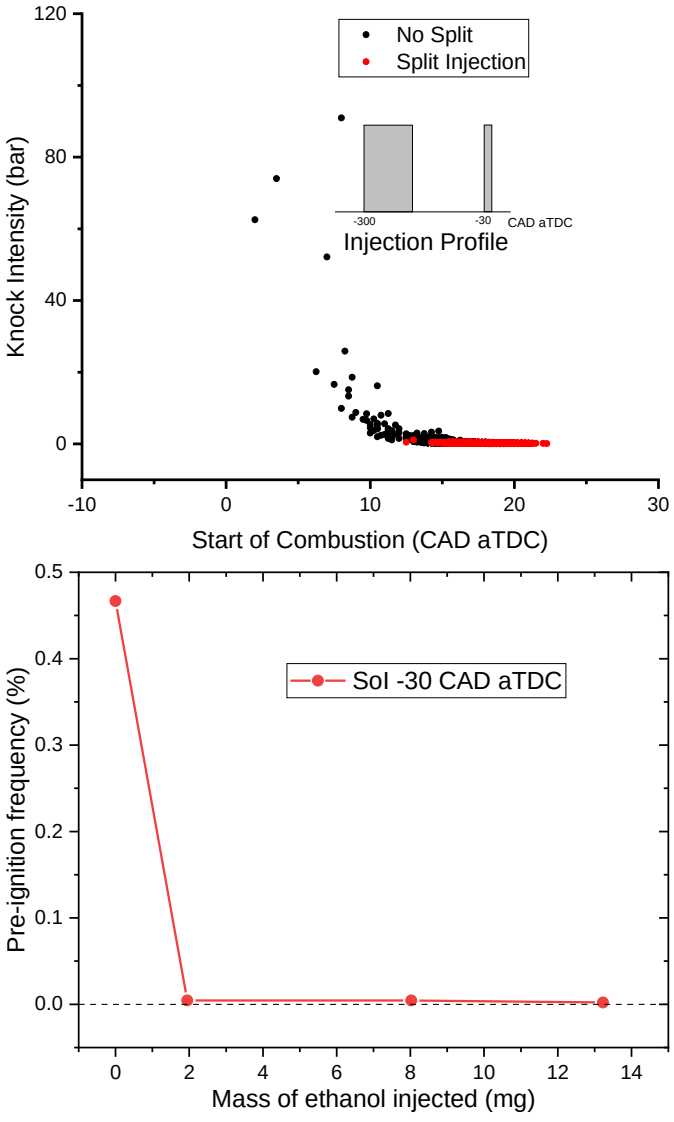

Figure 12: (a) Split injection strategy is shown wherein major fraction of the fuel is injected early in intake stroke (-300 CAD aTDC) and a small fraction is injected late in compression stroke (-30 CAD aTDC). (b) Gasoline in the late injection pulse (-30 CAD aTDC) is replaced with ethanol while the main fuel (injected at -300 CAD aTDC) is still gasoline [27, 28].

Overall, using ethanol in blend increased pre-ignition frequency. However, by injecting ethanol separately, as in the Octane-on-Demand concept or direct fuel injection close to TDC, pre-ignition frequency can be reduced owing to the reduction in fuel from direct injection and charge cooling benefits of ethanol. The current study looked at fuel effects on pre-ignition, as opposed to the lubricant effect, which is currently investigated extensively by researchers across the globe [2, 53-60]. A fuel and lubricant agnostic method to avoid the potential damage from a pre-ignition event can be the detection of pre-ignition early in the combustion cycle and triggering an evasive action. Such sensors have been developed by our team and fuel enrichment and counter spark to burn the end-gas (before super-knock) have been investigated in separate studies of interest [61, 62].

Conclusions:

This study focused on studying the combustion behavior of ethanol blended in gasolines. Experiments in IQT ascertained the ethanol required to blend in various FACE fuels to match their ignition delay times. Although the fuels showed similar ignition delay times in stratified combustion mode, their auto-ignition tendency in homogeneous combustion mode was slightly different. FACE G showed the least auto-ignition tendency, followed by FACE A and FACE C blended with 13% (v/v) ethanol, followed by FACE I and FACE J blended with 27% (v/v) ethanol. In terms of pre-ignition frequency, increasing ethanol fraction led to increase in pre-ignition frequency. For blends with the same ethanol fraction, FACE fuels with higher aromatics led to higher pre-ignition frequency. The study further establishes the distinction between pre-ignition and super-knock (auto-ignition of end-gas), as the blends showing highly disparate pre-ignition frequency showed similar auto-ignition tendency in HCCI and SI operation.

Acknowledgment:

The project is part of FUELCOM II. The authors acknowledge the funding agency Saudi Aramco for financial assistance. The authors thank Adrian Ichim, for his technical support in conducting experiments. The authors would like to thank the contribution of Monika Priyadarshini for figure 11 of the manuscript.

References:

[1] E. Chapman, R. S. Davis, W. Studzinski, and P. Geng, "Fuel octane and volatility effects on the stochastic pre-ignition behavior of a 2.0 L gasoline turbocharged DI engine," SAE International Journal of Fuels and Lubricants, vol. 7, no. 2014-01-1226, pp. 379-389, 2014.

[2] V. S. Costanzo, X. Yu, E. Chapman, R. Davis, and P. Haenel, "Fuel & Lubricant Effects on Stochastic Preignition," SAE Technical Paper 2019-01-0038, 2019.

[3] E. Singh, M. J. M. Ali, A. Ichim, K. Morganti, and R. Dibble, "Effect of Mixture Formation and Injection Strategies on Stochastic Pre-Ignition," SAE Technical Paper 2018-01-1678, 2018.

[4] A. Michlberger, M. Sutton, M. Kocsis, G. Anderson, and A. Van Horn, "On-Road Monitoring of Low Speed Pre-Ignition," SAE Technical Paper 2018-01-1676, 2018.

[5] D. Downs and J. Pigneguy, "An experimental investigation into pre-ignition in the spark-ignition engine," Proceedings of the Institution of Mechanical Engineers: Automobile Division, vol. 4, no. 1, pp. 125-149, 1950.

[6] D. Downs and F. Theobald, "The effect of fuel characteristics and engine operating conditions on pre-ignition," Proceedings of the Institution of Mechanical Engineers: Automobile Division, vol. 178, no. 1, pp. 89-108, 1963.

[7] I. Zeldovich, G. I. Barenblatt, V. Librovich, and G. Makhviladze, "Mathematical theory of combustion and explosions," 1985.

[8] G. Kalghatgi, "Fuel/Engine Interactions," ed: SAE International, 2013.

[9] G. Kalghatgi, I. Algunaibet, and K. Morganti, "On Knock Intensity and Superknock in SI Engines," SAE International Journal of Engines, vol. 10, no. 2017-01-0689, 2017.

[10] G. T. Kalghatgi and D. Bradley, "Pre-ignition and 'super-knock'in turbo-charged spark-ignition engines," International Journal of Engine Research, vol. 13, no. 4, pp. 399-414, 2012.

[11] T. Hülser, G. Grünefeld, T. Brands, M. Günther, and S. Pischinger, "Optical investigation on the origin of pre-ignition in a highly boosted SI engine using bio-fuels," SAE Technical Paper 2013-01-1636, 2013.

[12] M. Mayer, P. Hofmann, B. Geringer, J. Williams, J. Moss, and P. Kapus, "Influence of different oil properties on low-speed pre-ignition in turbocharged direct injection spark ignition engines," SAE Technical Paper 2016-01-0718, 2016.

[13] C. Martin, J. Graf, B. Geringer, R. Luef, P. Grabner, and H. Eichlseder, "Neue Prüfmethodiken des Klopfens und der Vorentflammung von Kraftstoffen und Ölen hochaufgeladener Ottomotoren," in Internationales Wiener Motorensymposium= International Vienna Motor Symposium, 2014, pp. 236-265: Springer-VDI-Verlag GmbH & Co. KG.

[14] P. Haenel, H. Kleeberg, R. de Bruijn, and D. Tomazic, "Influence of Ethanol Blends on Low Speed Pre-Ignition in Turbocharged, Direct-Injection Gasoline Engines," SAE International Journal of Fuels and Lubricants, vol. 10, no. 2017-01-0687, pp. 95-105, 2017.

[15] C. Dahnz and U. Spicher, "Irregular combustion in supercharged spark ignition engines–pre-ignition and other phenomena," International Journal of Engine Research, vol. 11, no. 6, pp. 485-498, 2010.

[16] Y. He, Z. Liu, I. Stahl, G. Zhang, and Y. Zheng, "Comparison of stochastic pre-ignition behaviors on a turbocharged gasoline engine with various fuels and lubricants," SAE Technical Paper 2016-01-2291, 2016.

[17] N. Sasaki and K. Nakata, "Effect of Fuel Components on Engine Abnormal Combustion," 2012. Available: http://dx.doi.org/10.4271/2012-01-1276

[18] N. Sasaki, K. Nakata, K. Kawatake, S. Sagawa, M. Watanabe, and T. Sone, "The Effect of Fuel Compounds on Pre-ignition under High Temperature and High Pressure Condition," 2011. Available: http://dx.doi.org/10.4271/2011-01-1984

[19] A. B. Mansfield, E. Chapman, and K. Briscoe, "Effect of market variations in gasoline composition on aspects of stochastic pre-ignition," Fuel, vol. 184, pp. 390-400, 2016.

[20] R. Perry, P. Gerard, and D. Heath, "The Influence of Gasoline Composition on Abnormal Combustion in Spark Ignition Engines," SAE Technical Paper 610145, 1961.

[21] N. Naser, A. G. A. Jameel, A.-H. Emwas, E. Singh, S. H. Chung, and S. M. Sarathy, "The influence of chemical composition on ignition delay times of gasoline fractions," Combustion and Flame, vol. 209, pp. 418-429, 2019.

[22] N. Naser, S. Y. Yang, G. Kalghatgi, and S. H. Chung, "Relating the octane numbers of fuels to ignition delay times measured in an ignition quality tester (IQT)," Fuel, vol. 187, pp. 117-127, 2017.

[23] D. ASTM, "6890 Standard Test Method for Determination of Ignition Delay and Derived Cetane Number (DCN) of Diesel Fuel Oils by Combustion in a Constant Vol," ed: Chamber, 2011.

[24] D. ASTM, "2699, Standard Test Method for Research Octane Number of Spark-Ignition Engine Fuel," American Society for Testing and Materials (ASTM), 2013.

[25] D. ASTM, "2700, Standard Test Method for Motor Octane Number of Spark-Ignition Engine Fuel," American Society for Testing and Materials (ASTM), 2014.

[26] E. Singh, M. Waqas, B. Johansson, and M. Sarathy, "Simulating HCCI Blending Octane Number of Primary Reference Fuel with Ethanol," SAE Technical Paper 2017-01-0734, 2017.

[27] E. Singh, P. Hlaing, H. Shi, and R. Dibble, "Effect of Different Fluids on Injection Strategies to Suppress Pre-Ignition," SAE Technical Paper 2019-01-0257, 2019.

[28] E. Singh, K. Morganti, and R. Dibble, "Optimizing split fuel injection strategies to avoid pre-ignition and super-knock in turbocharged engines," International Journal of Engine Research, p. 1468087419836591, 2019.

[29] J.-M. Zaccardi, L. Duval, and A. Pagot, "Development of Specific Tools for Analysis and Quantification of Pre-ignition in a Boosted SI Engine," 2009.

[30] A. International, "ASTM D86, Standard Test Method for Distillation of Petroleum Products at Atmospheric Pressure," ed: ASTM International West Conshohocken, PA, 2004.

[31] N. Naser, S. M. Sarathy, and S. H. Chung, "Estimating fuel octane numbers from homogeneous gas-phase ignition delay times," Combustion and Flame, vol. 188, pp. 307-323, 2018.

[32] E. Singh, E. Tingas, D. Goussis, H. G. Im, and S. M. Sarathy, "Chemical ignition characteristics of ethanol blending with primary reference fuels," Energy & Fuels, 2019.

[33] A. A. Ahmed, A. M. El-Masry, and Y. Barakat, "Azeotrope formation in gasoline–ethanol blends. Part 1–Impact of nonionic on E10 distillation curve," Egyptian journal of petroleum, vol. 27, no. 4, pp. 1167-1175, 2018.

[34] Standard Specification for Automotive Spark-Ignition Engine Fuel.

[35] V. F. Andersen, J. Anderson, T. Wallington, S. Mueller, and O. J. Nielsen, "Distillation curves for alcohol− gasoline blends," Energy & Fuels, vol. 24, no. 4, pp. 2683-2691, 2010.

[36] R. M. Balabin, R. Z. Syunyaev, and S. A. Karpov, "Quantitative Measurement of Ethanol Distribution over Fractions of Ethanol− Gasoline Fuel," Energy & fuels, vol. 21, no. 4, pp. 2460-2465, 2007.

[37] M. Waqas, N. Naser, M. Sarathy, K. Morganti, K. Al-Qurashi, and B. Johansson, "Blending Octane Number of Ethanol in HCCI, SI and CI Combustion Modes," SAE International Journal of Fuels and Lubricants, vol. 9, no. 2016-01-2298, pp. 659-682, 2016.

[38] G. Gentz, J. Dernotte, C. Ji, D. Lopez Pintor, and J. Dec, "Combustion-Timing Control of Low-Temperature Gasoline Combustion (LTGC) Engines by Using Double Direct-Injections to Control Kinetic Rates," 2019. Available: https://doi.org/10.4271/2019-01-1156

[39] G. Gentz, J. Dernotte, C. Ji, and J. Dec, "Spark Assist for CA50 Control and Improved Robustness in a Premixed LTGC Engine – Effects of Equivalence Ratio and Intake Boost," 2018. Available: https://doi.org/10.4271/2018-01-1252

[40] R. Design, "CHEMKIN-PRO," ed: Reaction Design San Diego, CA, 2008.

[41] A. Ahmed, G. Goteng, V. S. Shankar, K. Al-Qurashi, W. L. Roberts, and S. M. Sarathy, "A computational methodology for formulating gasoline surrogate fuels with accurate physical and chemical kinetic properties," Fuel, vol. 143, pp. 290-300, 2015.

[42] S. M. Sarathy et al., "Compositional effects on the ignition of FACE gasolines," Combustion and Flame, vol. 169, pp. 171-193, 2016.

[43] T. Javed et al., "Ignition studies of two low-octane gasolines," Combustion and Flame, vol. 185, pp. 152-159, 2017.

[44] E. Singh, J. Badra, M. Mehl, and S. M. Sarathy, "Chemical Kinetic Insights into the Octane Number and Octane Sensitivity of Gasoline Surrogate Mixtures," Energy & Fuels, vol. 31, no. 2, pp. 1945-1960, 2017.

[45] E. Singh and R. Dibble, "Mechanism triggering pre-ignition in turbo-charged engines," SAE Technical Paper 2019-01-0255, 2019.

[46] K. Morganti et al., "Synergistic engine-fuel technologies for light-duty vehicles: Fuel economy and Greenhouse Gas Emissions," Applied Energy, vol. 208, pp. 1538-1561, 2017.

[47] K. Morganti, M. Al-Abdullah, and A. Zubail, "Fuel economy and CO2 emissions benefits of octane-on-demand combustion in spark-ignition engines," Carbon, vol. 1, no. 2.18, p. 2.24, 2015.

[48] K. Morganti, M. Almansour, A. Khan, G. Kalghatgi, and S. Przesmitzki, "Leveraging the benefits of ethanol in advanced engine-fuel systems," Energy Conversion and Management, vol. 157, pp. 480-497, 2018.

[49] K. Morganti et al., "Improving the Efficiency of Conventional Spark-Ignition Engines Using Octane-on-Demand Combustion-Part II: Vehicle Studies and Life Cycle Assessment," SAE Technical Paper 2016-01-0683, 2016.

[50] K. Morganti, Y. Viollet, R. Head, G. Kalghatgi, M. Al-Abdullah, and A. Alzubail, "Maximizing the benefits of high octane fuels in spark-ignition engines," Fuel, vol. 207, pp. 470-487, 2017.

[51] E. Singh, Morganti, K., Dibble, R. W., "Dual-fuel operation of Gasoline and Natural Gas in a Turbocharged Engine.," FUEL, 2018.

[52] E. Singh, K. Morganti, and R. Dibble, "Knock and Pre-Ignition Limits on Utilization of Ethanol in Octane-on-Demand Concept," SAE Technical Paper 2019-24-0108, 2019.

[53] S. F. Dingle, A. Cairns, H. Zhao, J. Williams, O. Williams, and R. Ali, "Lubricant induced pre-ignition in an optical SI engine," SAE Technical Paper 2014-01-1222, 2014.

[54] K. A. Fletcher, L. Dingwell, K. Yang, W. Y. Lam, and J. P. Styer, "Engine Oil Additive Impacts on Low Speed Pre-Ignition," SAE International Journal of Fuels and Lubricants, vol. 9, no. 2016-01-2277, pp. 612-620, 2016.

[55] M. C. Kocsis, T. Briggs, and G. Anderson, "The impact of lubricant volatility, viscosity and detergent chemistry on low speed pre-ignition behavior," SAE International Journal of Engines, vol. 10, no. 2017-01-0685, pp. 1019-1035, 2017.

[56] S. Park, S. Woo, H. Oh, and K. Lee, "Effects of Various Lubricants and Fuels on Pre-Ignition in a Turbocharged Direct-Injection Spark-Ignition Engine," Energy & Fuels, vol. 31, no. 11, pp. 12701-12711, 2017.

[57] O. Welling, N. Collings, J. Williams, and J. Moss, "Impact of lubricant composition on low-speed pre-ignition," SAE Technical Paper 2014-01-1213, 2014.

[58] O. Welling, J. Moss, J. Williams, and N. Collings, "Measuring the impact of engine oils and fuels on low-speed pre-ignition in downsized engines," SAE International Journal of Fuels and Lubricants, vol. 7, no. 2014-01-1219, pp. 1-8, 2014.

[59] Y. Moriyoshi, T. Yamada, D. Tsunoda, M. Xie, T. Kuboyama, and K. Morikawa, "Numerical simulation to understand the cause and sequence of LSPI phenomena and suggestion of CaO mechanism in highly boosted SI combustion in low speed range," SAE Technical Paper 2015-01-0755, 2015.

[60] S. Maharjan, Y. Qahtani, W. Roberts, and A. Elbaz, "The Effect of Pressure, Temperature and Additives on Droplet Ignition of

Lubricant Oil and Its Surrogate," 2018. Available: https://doi.org/10.4271/2018-01-1673

[61] E. Singh and R. Dibble, "Effectiveness of Fuel Enrichment on Knock Suppression in a Gasoline Spark-Ignited Engine," SAE Technical Paper 2018-01-1665, 2018.

[62] D. S. Roberts, Eshan; Morganti, Kai; Raman, Vallinayagam, "Internal Combustion Engines having Super-knock Mitigation controls and methods for their operation.," Saudi Arabia, 2019.

Definitions/Abbreviations

API	American Petroleum Institute
ASTM	American Society for Testing and Materials
aTDC	After top dead center
CA05	Crank Angle for 5% of total heat released
CA50	Crank Angle for 50% of total heat released
CAD	Crank angle degrees
CFR	Co-operative Fuel Research
DHA	Detailed Hydrocarbon Analysis
DOHC	Direct overhead cam
FACE	Fuels for Advanced Combustion Engines
GHG	Greenhouse Gases
HCCI	Homogeneous Charge Compression Ignition
IDT	Ignition Delay Time
IMEP	Indicated Mean Effective Pressure
IQT	Ignition Quality Tester
MBT	Maximum Brake Torque
MON	Motor Octane Number
NTC	Negative Temperature Coefficient
PFI	Port Fuel Injection
RON	Research Octane Number
rpm	Rotations per minute
S	Octane Sensitivity (RON-MON)
SI	Spark Ignition

Contact Information

Eshan Singh
Clean Combustion Research Centre
King Abdullah University of Science and Technology
Thuwal, Saudi Arabia
eshan.singh@kaust.edu.sa
+966 544 511 843